ELSEVIER

Contents lists available at ScienceDirect

International Journal of Heat and Mass Transfer

journal homepage: www.elsevier.com/locate/ijhmt



Cryoprotective mechanism of using Ficoll for cell cryopreservation at non-cryogenic temperatures: A molecular dynamics study



Yijin Mao^a, Xu Han^{a,b,*}, Yuwen Zhang^{a,*}

- ^a Department of Mechanical and Aerospace Engineering, University of Missouri, Columbia, MO 65211, USA
- ^b CryoCrate LLC, 1601 S. Providence Rd., Columbia, MO 65211, USA

ARTICLE INFO

Article history:
Received 25 April 2018
Received in revised form 27 June 2018
Accepted 28 June 2018
Available online 14 July 2018

Keywords: Cryoprotective mechanism Non-cryogenic temperature Recrystallization Molecular dynamics Firoll

ABSTRACT

Molecular dynamics simulations were carried out to investigate the cryoprotective mechanism of using Ficoll, a highly compact spherical polysucrose, as a non-permeating cryoprotectant for practices of cell cryopreservation at temperatures higher than -80 °C. Three types of simulation boxes were prepared for Ficoll-dimethyl sulfoxide (DMSO)-water, sucrose-DMSO-water, and DMSO-water systems, respectively, and depicted with the Optimized Potentials for Liquid Simulations (OPLS-all) as potential function for molecular systems. The entire molecular system for each scenario was firstly fully equilibrated into a state with known concentration, density and temperature, in agreement with the corresponding existing or newly measured phase-diagrams. Thereafter, molecular dynamics simulations were performed to characterize the behavior of liquid water molecules surrounding a pre-sited ice nucleus that was placed at the center of each molecular system by calculating the radial density distribution (RDF) and root-mean-square distance (RMSD) of atomic positions. The results showed that the system with Ficoll molecules present behaved significantly different from the other two systems at various non-cryogenic temperatures (-10 °C, -20.3 °C, -33.9 °C, and -80 °C). The Ficoll molecules obviously prevent the water molecules from approaching the ice nuclei, and simultaneously lower the activities of the water molecules. These results agree well with previous thermal studies that demonstrate the effect of using Ficoll to minimize recrystallization of such solutions, and also provide a qualitative explanation on a molecular level for why Ficoll facilitates long-term storage of cells at non-cryogenic temperatures.

© 2018 Elsevier Ltd. All rights reserved.

1. Introduction

With recent advances in development of cell-based therapy, tissue engineering and regenerative medicine technologies for biomedical applications, there has always been an urgent need in improving the cryopreservation efficiency for large stocks of cell and tissue [1–3]. Traditional cryopreservation media contain primarily cell membrane permeating cryoprotectants, e.g., dimethyl sulfoxide (DMSO), ethylene glycol, and 1,2-propanediol, plus low concentrations of non-permeating small molecular or polymer cryoprotectants (e.g., sucrose, trehalose, polyvinylpyrrolidone, and polyethylene glycol). These solutions are thermally unstable when frozen at non-cryogenic temperatures, e.g., –80 °C, and the recrystallization temperature of the unfrozen portion of those solutions is generally higher than –100 °C [4–7]. Since recrystallization

E-mail addresses: hanx@missouri.edu (X. Han), zhangyu@missouri.ed (Y. Zhang).

causes severe mechanical damage to cells [4–7], current long term cryopreservation of cell stocks routinely requires the use of liquid nitrogen and associated facilities to provide a temperature range for safe storage between approximately $-120\,^{\circ}\text{C}$ (the temperature of the vapor phase in Dewar or cryogenic freezers) and $-196\,^{\circ}\text{C}$ (the saturation temperature) to prevent recrystallization during storage.

However, the frequent use of liquid nitrogen is a heavy financial burden and requires the construction of safe but expensive liquid nitrogen supply systems. The associated operating procedures (e.g., sample loading and collection, liquid nitrogen refilling and storage tank cleaning, handling and shipping) are time consuming and laborious, with numerous safety and maintenance issues also generated (e.g., cold burn and asphyxiation). Based on previous differential scanning calorimetric experimental investigations [8], we discovered that using a low concentration (typically 10% w/w) of a highly compact spherical polysaccharide, Ficoll 70 (also called polysucrose 70 by some manufacturers), significantly increases the recrystallization temperatures of cryopreservation media to a much greater extent than use of normal non-permeating or

^{*} Corresponding authors at: Department of Mechanical and Aerospace Engineering, University of Missouri, Columbia, MO 65211, USA (X. Han and Y. Zhang).

E-mail addresses: hanx@missouri.edu (X. Han), zhangyu@missouri.edu

Nomenclature Lennard-Jones parameters, N m¹³ Α time, s C Lennard-Jones parameters, N m⁷ V energy, I e electron charge x position, m Е energy, J f fudge factor Greek symbols K spring constant, N/m or N/rad distance, m q charge on each atom, electron dielectric constant, F/m ϵ r position, m θ angle, ° r distance, m angle. °

polymer cryoprotectants (e.g. sucrose and polyvinylpyrrolidone) of similar concentrations. This invention enables long-term storage of mammalian and insect cells in regular deep freezers operating at $-70\,^{\circ}\mathrm{C}$ to $-85\,^{\circ}\mathrm{C}$ with the post-thaw viability and functionality comparable to those from the standard storage protocol using liquid nitrogen facilities, and thereby significantly improves the efficacy of cell cryopreservation and biobanking [8,9]. We hypothesized that the highly compact structure and highly hydrophilic surface of Ficoll molecules play critical roles in modification of the recrystallization processes, and subsequently carried out molecular dynamics to validate our hypothesis in this study.

The method of molecular dynamics is widely recognized as a powerful and cost-effective computational technique that is capable of providing preliminary views to reveal the mechanism of ice growth from a perspective on the molecular level [10–13]. Hence, this method offered highly valuable information for exploring the potentials of innovative non-permeating cryoprotectants, e.g., xenon gas, trehalose, antifreeze proteins and their analogues, by revealing the associated cryoprotective mechanism [14–19]. However, the recrystallization process of partially frozen solutions generally takes days or weeks at low temperatures, which is far beyond existing computational capabilities if a normal molecular dynamic simulation strategy is applied.

In this study, to overcome these technical challenges, we created a novel model, namely, "inserting" an ice nucleus into each of the simulation boxes for the unfrozen portion of cryoprotectant solutions equilibrating at certain temperatures, and then characterized the water molecule behaviors to predict the recrystallization potentials. We studied and compared the Ficoll-DMSO-water, sucrose-DMSO-water, and DMSO-water systems. To provide the concentration and temperature information for the calculations, we also measured the phase diagram of the Ficoll-DMSO-water system using differential scanning calorimetry, and applied existing phase diagrams of DMSO-water and sucrose-DMSO-water systems.

2. Molecular dynamics simulation

In the present simulations, complex molecular systems, Ficoll-DMSO-water, DMSO-water, and sucrose-DMSO-water system are investigated at given temperatures and concentrations to reveal how Ficoll molecule distinguishes from the others and further improve recrystallization behavior. In order to appropriately describe the molecular system, a standard and optimized potential (OPLS-aa) [20,21] was directly adopted by the liquid simulation force field to describe the molecular systems. Namely, the energy of the system was described as.

$$E(\mathbf{r}) = E_{bonds} + E_{angles} + E_{dihedrals} + E_{non-bonded} \tag{1}$$

where the energy contribution to the bonds was

$$E_{bonds} = \sum_{bonds} K_r (r - r_0)^2 \tag{2}$$

The energy contribution to the angles was

$$E_{angles} = \sum_{angles} K_{\theta} (\theta - \theta_0)^2 \tag{3}$$

The energy contribution to the dihedrals was

$$\begin{split} E_{dihedrals} &= \sum_{dihedrals} \left(\frac{V_1}{2} [1 + \cos(\phi - \phi_0)] + \frac{V_2}{2} [1 - \cos 2(\phi - \phi_0)] \right) \\ &+ \sum_{dihedrals} \left(\frac{V_3}{2} [1 + \cos 3(\phi - \phi_0)] + \frac{V_4}{2} [1 - \cos 4(\phi - \phi_0)] \right) \end{split}$$
(4)

And the energy contribution to the non-bonded was

$$E_{non-bonded} = \sum_{i>j} f_{ij} \left(\frac{A_{ij}}{r_{ij}^{12}} - \frac{C_{ij}}{r_{ij}^{6}} + \frac{q_i q_j e^2}{4\pi \varepsilon_0 r_{ij}} \right)$$
 (5)

According to the methodology described in [21,22], the nonbonded energy was counted for atoms with three or more bonds apart, and the 1, 4 interactions was scaled down by the fudge factor f_{ii} of 0.5 for the intramolecular non-bonded interactions. The geometric rule was assumed for the pair-wise interaction between different atoms. The structures of different molecules are illustrated in Fig. 1(a)-(d), for DMSO, Sucrose, Ficoll 70 and water, respectively. In the previous studies [8], we found that Ficoll 70 is more efficient in prevention of recrystallization than Ficoll 400, because the solutions of Ficoll 70 recrystallize at higher temperature than those of Ficoll 400 when their concentrations are the same, so we chose Ficoll 70 in all cases. Since the Ficoll 70 molecule is neutral, highly branched and compact, and also a spherical polymer of sucrose molecules, then the Ficoll structure in the current model was approximated by organizing a linear chain of sucrose molecules to form a neutrally charged and compact spherical structure with a diameter of approximately 5 nm [23]. The molecular weight (MW) of each constructed Ficoll molecule approaches 70 kg/mole, i.e. the mean MW of mass produced Ficoll 70. The parameters of non-bonded interaction for these molecules are given in the Table 1 [24]. The parameters for the bond/angle/dihedral of each molecule structure were determined based on the types of atoms and through the use of an existing tool, moltemplate [25]. Three types of simulation boxes for molecular systems, namely, Ficoll 70-DMSO-water, Sucrose-DMSO-water, and DMSO-water, were prepared for the molecular dynamics simulations. It is worthwhile pointing out that SPC water model is applied rather than TIP4P/ Ice in the consideration of the objective of present study that is investigating the water molecule's activities surrounding the ice nucleus. The conclusion of the study stay valid as long as the same water model is employed for all molecular systems. In addition, three-site model demands less computational resources than that of four-, five-, or six-site models due to its geometrical simplicity. To enable molecular dynamics to study the time-consuming recrystallization process, we deployed the following strategy.

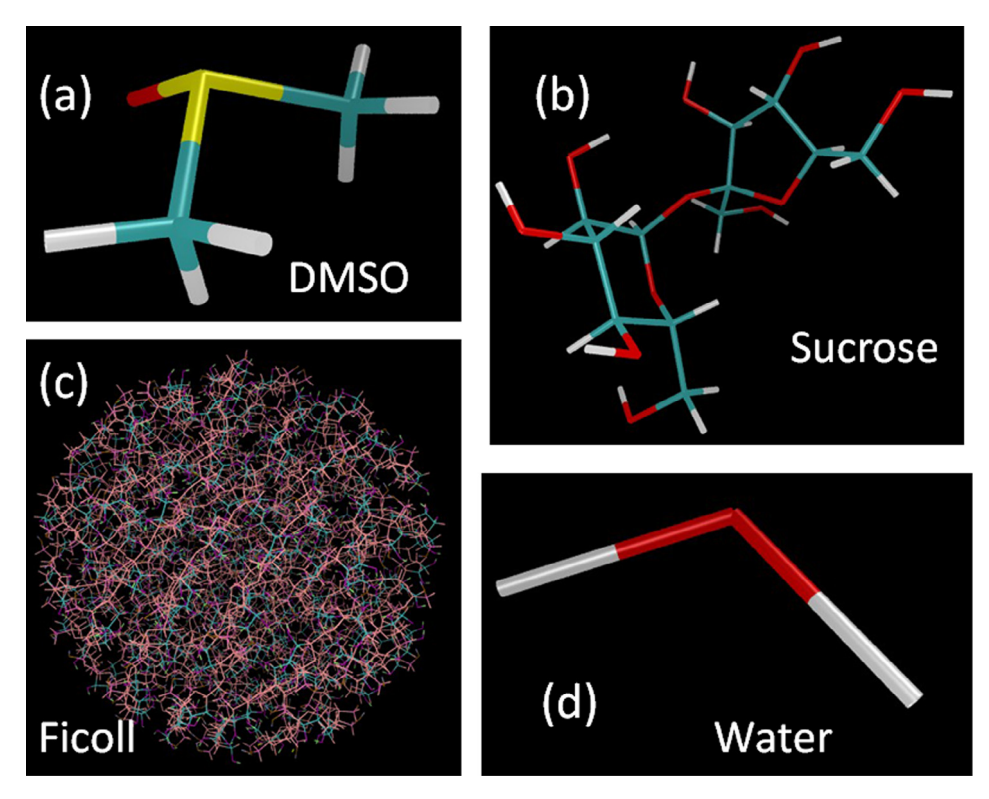


Fig. 1. Visualization of the constructed molecule structures.

Table 1Parameters for the non-bonded pairwise potentials.

Atom type	mass (g/mole)	ε (kcal/mol)	σ(Å)	q (e)
SPC water O	15.999	0.1554	3.16557	-0.82
SPC water H	1.008	0.0	0.0	0.41
Alkane H-C	1.008	0.03	2.5	0.06
Alcohol —OH	15.999	0.17	3.12	-0.683
Alcohol —OH	1.008	0.0	0.0	0.418
Alcohol CH3OH & RCH2OH	12.011	0.066	3.5	0.145
Alcohol R2CHOH	12.011	0.066	3.5	0.205
Diol —OH	15.999	0.17	3.07	-0.7
Diol —OH	1.008	0.0	0.0	0.435
Triol -OH	15.999	0.17	3.07	-0.73
Triol —OH	1.008	0.0	0.0	0.465
Diol & triol -CHROH	12.011	0.066	3.5	0.205
Diol & triol H-COH	1.008	0.03	2.5	0.06
Dialkyl ether —O—	15.999	0.14	2.9	-0.4
Ethyl ether —CH2OR	12.011	0.066	3.5	0.14
Isopropyl ether >CHOR	12.011	0.066	3.5	0.17
Alkyl ether H-COR	1.008	0.03	2.5	0.03
Acetal RO-CR2OX	15.999	0.14	2.9	-0.4
Acetal RO-CHR-OR	12.011	0.066	3.5	0.3
Acetal RO-CHR-OR	1.008	0.03	2.5	0.1
Acetal RO-CR2-OR	12.011	0.066	3.5	0.4
Dialkyl sulfoxide	32.06	0.395	3.56	0.13
Sulfoxide R-SO-R	15.999	0.28	2.93	-0.42
Sulfoxide CH3-SO-R	12.011	0.066	3.5	-0.035

The construction of each simulation box was based on the information of the concentration and temperature values of the corresponding phase-diagram. The binary phase diagram of DMSO-water and the ternary phase diagram of sucrose-DMSO-water were available [26,27]. Using differential scanning calorimetry and based on our previous work [28], we measured the partial ternary phase diagram of Ficoll-DMSO-water using a mass redemption method to improve the accuracy and efficiency, and the results are shown in Fig. 2. All these data provided us with accurate information (5% or less as the relative error) for the

weight concentration values of solutes at the corresponding equilibrating temperature [28]. For the Ficoll 70-DMSO-water system, we successfully achieved long-term storage of stem cells at $-80\,^{\circ}\text{C}$ using 10% (w/w) Ficoll and 10% DMSO [8], so the value of the weight ratio between Ficoll 70 and DMSO was chosen as 1:1 (i.e., R = 1.0 in Fig. 2) for the following simulations. The data on the curve with R as 1.0 in Fig. 2 were then used. Therefore, at the storage temperature, i.e. $-80\,^{\circ}\text{C}$, based on the extrapolation from the data in Fig. 2, we approximated the equilibrated ternary Ficoll 70-DMSO-water system (with the weight ratio between Ficoll 70

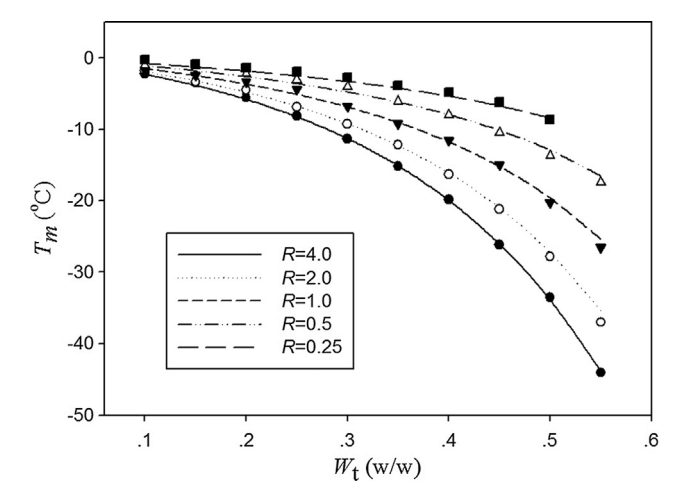


Fig. 2. Partial phase diagram of the Ficoll 70-DMSO-water system using differential scanning calorimetry and the method described in our previous work [28]: Tm is the melting point, R is the weight ratio between DMSO and Ficoll 70, and Wt is the total weight percentage of both solutes, i.e. DMSO and Ficoll 70, of the solutions; the fitting curves were made using the formulas described previously [28].

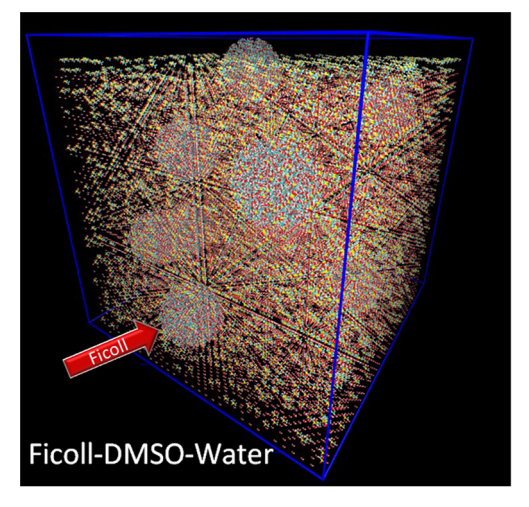
Table 2The specifications of the six simulation boxes used in this study. The numbers of the molecules were determined based the phase diagram data for the Ficoll 70-DMSO-water system (shown in Fig. 2), sucrose-DMSO-water system [27], and DMSO-water system [26].

Systems	Equilibrium temperature	Numbers of the molecules	Size of the simulation box (Å ³)
Ficoll 70- DMSO- water Sucrose-	-80 °C -80 °C	Ficoll 70: 8 DMSO: 7,344 Water: 27,496 Sucrose: 7,788	156.93 × 159.48 × 159.30 163.53 × 169.88 ×
DMSO- water DMSO-water	–80 °C	DMSO: 7,780 Water: 25,380 DMSO: 8,416	159.95 140.62 × 145.06 ×
		Water: 26,432	135.63
Ficoll 70- DMSO- water	−10 °C	Ficoll 70: 5 DMSO: 4,679 Water: 67,645	270.77 × 277.22 × 263.50
Ficoll 70- DMSO- water	−20.3 °C	Ficoll 70: 5 DMSO: 4,689 Water: 40,671	233.27 × 239.72 × 226.00
Ficoll 70- DMSO- water	−33.9 °C	Ficoll 70: 5 DMSO: 4,680 Water: 27,064	208.27 × 214.73 × 201.00

and DMSO as 1:1) by using a simulation box containing 8 Ficoll 70, 7,344 DMSO and 27,496 water molecules. Similarly, the number of molecules were determined for the DMSO-water binary system and the sucrose-DMSO-water ternary system. For the latter, the weight ratio between sucrose and DMSO was also chosen to be 1:1 for the comparison with the Ficoll 70-DMSO-water system. For the Ficoll 70-DMSO-water system, we also chose the cases equilibrated at the temperatures of $-10\,^{\circ}\text{C}, -20.3\,^{\circ}\text{C},$ and $-33.9\,^{\circ}\text{C}$ according to Fig. 2. The number values for different types of molecules and the sizes of these six systems are listed in Table 2. The initial molecular configuration of the atomistic system are shown in Fig. 3–5.

Based on the Eqs. (1)–(5), the molecular dynamic simulation was performed to determine the molecular distribution of these systems at their corresponding equilibrium states [26,27]. More specifically, the simulations were performed using the standard and widely accepted Large-scale Atomic/Molecular Massively Parallel Simulator (LAMMPS) [29], which is distributed by Sandia National Laboratories. The software VMD [30] was used to visualize the data as well as for data processing. Before the simulations were conducted, all these molecular systems were processed using an energy minimization procedure in order to determine an optimal initial configuration. Once the structure with a potentially minimum energy was found, the entire system was equilibrated at a state that presents the desired density and temperature. Each simulation was performed with approximately 154,000 steps for equilibrium and another 1,460,000 steps for data sampling within the same timestep of 1 fs.

A hexagonal ice nucleus containing 512 hexagonal ice unit cells was constructed based on the method described in [31,32]. The size of this ice nucleus varies during stabilizing process described below, but its maximum dimension is approximately 6 nm, and that is approximately the same as the size of ice critical nuclei in supercooled water estimated by previous molecular dynamic studies [33]. It was then "inserted" into the center of each equilibrated simulation box numerically, i.e., by replacing the same number of water molecules in the center of previously equilibrated systems. That structure was then treated as the starting point of the next round of the equilibrium process, performed as described above, to determine the new equilibrated distributions. To compare the potentials in recrystallization of these systems, we calculated both the radial density function (RDF) [34] and root-mean-square distance of atomic positions (RMSD) [24] of liquid water molecules. For the sake of increasing the comparability of the results from different molecular systems, Eq. (6) was utilized to calculate RMSD.



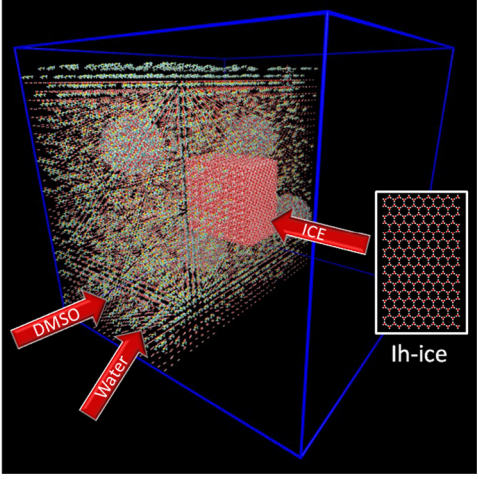


Fig. 3. Visualization of the simulation box for the Ficoll DMSO-water system at -80 °C with the ice nucleus placed at the center.

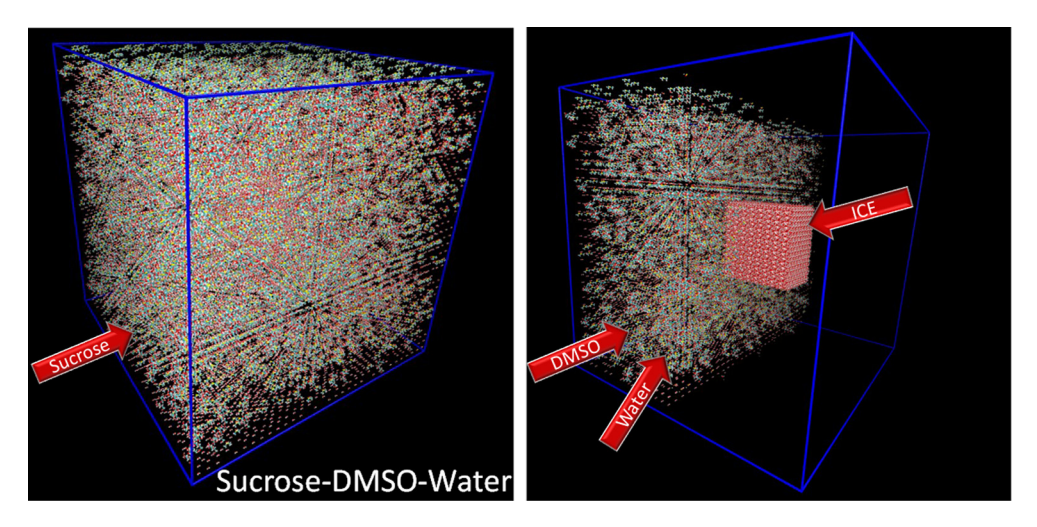


Fig. 4. Visualization of the simulation box for the sucrose-DMSO-water system at -80 °C with the ice nucleus placed at the center.

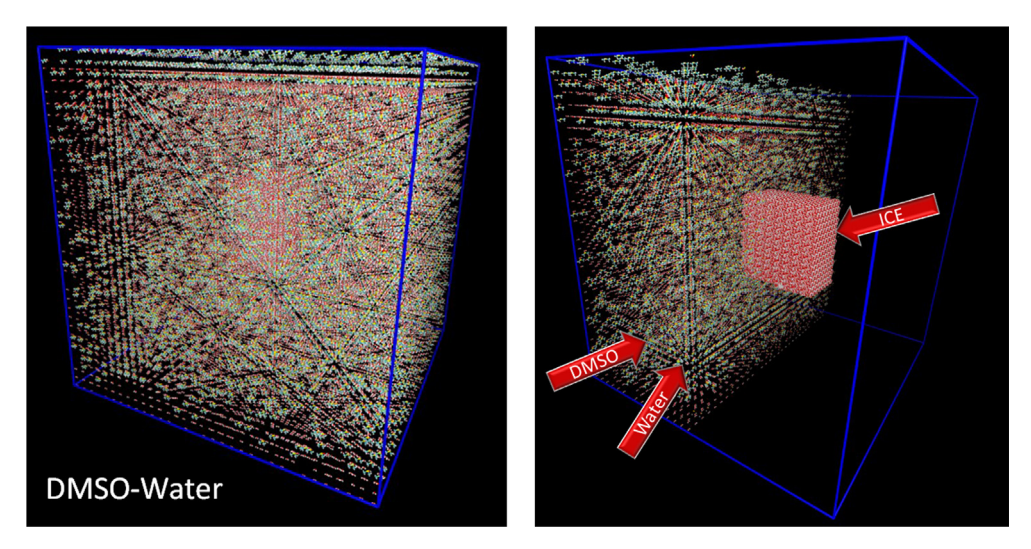


Fig. 5. Visualization of the simulation box for the DMSO-water system at -80 °C with the ice nucleus placed at the center.

$$\mathbf{RMSD}(t_n) = \sqrt{\frac{1}{N} \sum_{i}^{N} \delta_i^2} = \sqrt{\frac{1}{N} \sum_{i}^{N} [\mathbf{x}_i(t_n) - \mathbf{x}_i(t_{n-1})]^2}$$
 (6)

3. Results and discussions

Fig. 6 shows the results from RDF calculations for oxygen atoms of water molecules in the three simulation boxes equilibrated at -80 °C. As shown in Fig. 6, in the Ficoll 70-DMSO-water system, when compared with the other two systems, the presence of compact spherical Ficoll 70 molecules significantly increased the density of water molecules at a distance of approximately 40 Å from the center of the system. Figuratively speaking, the crowding of eight Ficoll 70 molecules in the system forms a "shell" of water molecules at that location, and strongly disrupts the relatively uniform distribution of water molecules presented in the other two systems at that particular range. In other words, the movement of the water molecules that approach the surface of an ice nucleus is hindered by the Ficoll molecules, most dramatically at the 40 Å location. We hence interpret this unique macromolecular crowding effect to be the reason that Ficoll 70 molecules are able to stabilize the ice crystals, and thereby prevent recrystallization at -80 °C. The physical mechanism of this effect may be related to the highly compact structure of Ficoll 70 molecules, and that alone

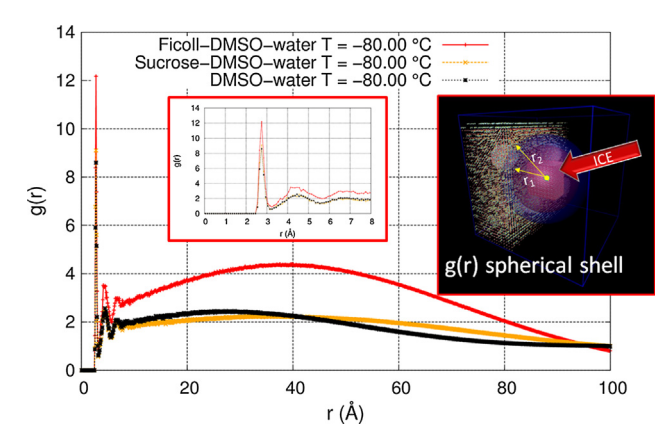


Fig. 6. Calculated radial density distribution of oxygen atoms in water molecules at -80 °C in the simulation boxes for different systems with the center of the ice nucleus as the origin (r = 0).

serves as a mechanical barrier to prevent ice growth. Alternatively, prevention of recrystallization may also be caused partially by the highly hydrophilic surface of the Ficoll 70 molecules. The spherical surface Ficoll 70 molecules is formed by branched sucrose

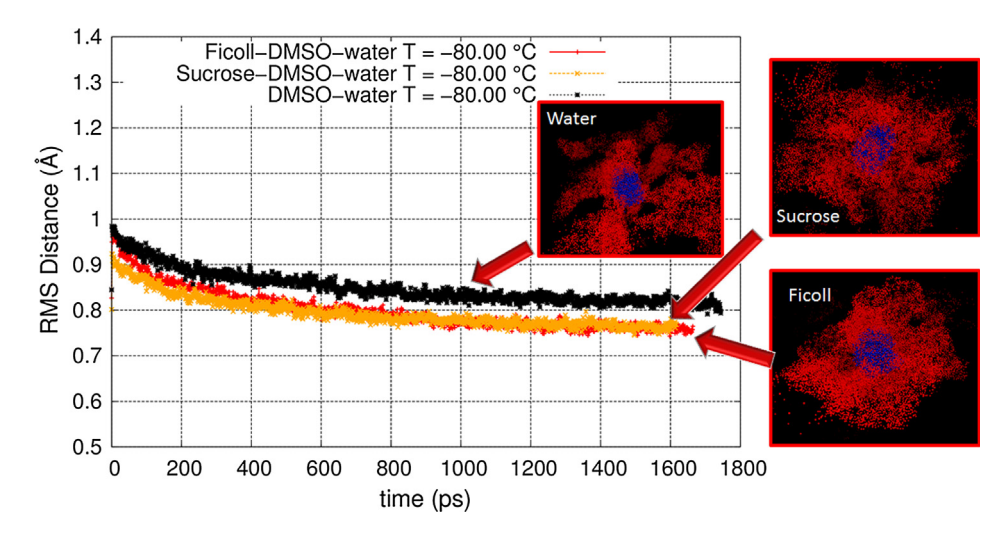


Fig. 7. Calculated Root-mean-square distance between oxygen atoms in water molecules at -80 °C in the simulation boxes for three different systems.

molecules with high hydrophilicity [23], and such characteristics would enable the macromolecules to slow water molecule displacement near its surface. Further theoretical and experimental investigations are required to provide a definitive and quantitative analyses. The influence of an artifact in our calculation should be noticed. As shown in Fig. 6, the first three peaks of the RDF curves located at 2.70 Å, 4.31 Å and 6.45 Å for all three systems, which is actually due to the influence of the presence of edges of the ice nucleus on the radial spacing of the RDF calculation. The difference in the sizes of the ice nuclei inserted to the simulation boxes will also influence the locations of the RDF peaks, but we expect that the same conclusion will be reached, i.e., the crowding of Ficoll molecules generates a certain RDF maximum which will be adjacent to the surface of the inserted nucleus.

The activity of liquid water molecules surrounding the ice nucleus was evaluated through the calculation of the RMSD of atomic positions of oxygen atoms of the water molecules. The results are shown in Fig. 7. Also shown are visualizations of final equilibrated structures of these three systems. The three RMSM curves show plateaus near the end of the calculations, and that indicate the systems were in an equilibrium state. We assume the activity of water molecules in the system is proportional to the value of RMSD [24]. Obviously, the traditional cryopreservation solution; namely, as DMSO-water binary system, shows the greatest activity of liquid water molecules among three systems. The RMSD values are very similar for Ficoll 70-DMSO-water and sucrose-DMSO-water systems, indicating that both Ficoll 70 and sucrose can reduce water activity. The primary reason for such reduced water activity is probably caused by the increase in viscosity. However, to achieve a similar effect, the use of relatively high weight ratios of sucrose in solutions does significantly increase the osmolality of the solutions, and thereby consequently causes osmotic damage to cells [35]. In contrast, for the Ficoll 70 solutions, even when the initial concentration of Ficoll 70 is as high as 10% w/ w, the osmolality increase is minimal due to the its high MW (see Fig. 2). Therefore, compared to the use of sucrose, the use of Ficoll 70, a highly compact polysucrose, is much preferred and more convenient for the purpose of cell cryopreservation.

Fig. 8 shows the comparison of the results from RDF calculations for the Ficoll 70-DMSO-water systems with the ice nucleus equilibrated at four different temperatures, i.e. $-10\,^{\circ}\text{C}$, $-20.3\,^{\circ}\text{C}$, $-33.9\,^{\circ}\text{C}$, and $-80\,^{\circ}\text{C}$. The RMSD values of the oxygen atoms in these systems are shown in Fig. 9. The four curves plateaued after 1200 ps, as shown in Fig. 9. Since all data were sampled at 1460 ps, then it is reasonable to conclude the systems were in their

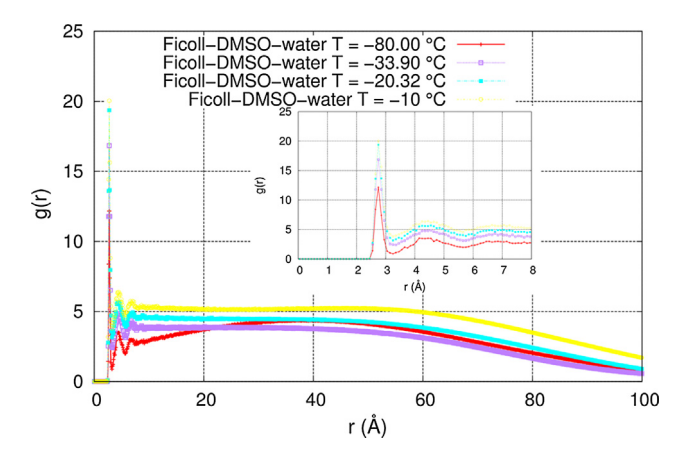


Fig. 8. Calculated radial density distribution of oxygen atoms in water molecules in the four different simulation boxes at different equilibrating temperatures (see Table 2) for the Ficoll 70-DMSO-water system, with the center of the ice nucleus as the origin (r = 0).

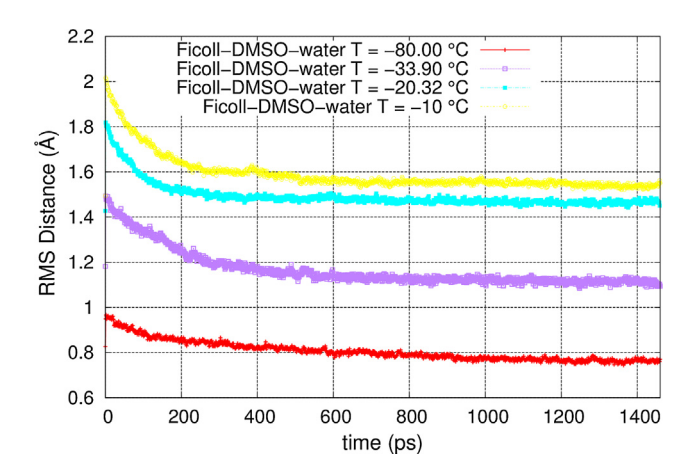


Fig. 9. Calculated root-mean-square distance of oxygen atom in water molecules in the four different simulation boxes at different equilibrating temperatures (see Table 2) for the Ficoll 70-DMSO-water system.

equilibrium states, and the results are valid. As shown in Fig. 9, the RMSD values, proportional to the kinetic energy of atoms, decrease as the temperature decreases. But the effects of Ficoll

70 on the modifying the shape of the RDF curves are similar. These results indicate that Ficoll 70 molecules also influence on recrystallization behavior of cryoprotectant solutions at higher temperatures. That effect is especially beneficial during the warming process, because if massive recrystallization occurs during warming, then the efforts in preventing recrystallization during storage would not result in satisfactory cell survival rates.

In summary, although the current molecular dynamics simulations may suffer inaccuracy due to the generality of the use of potential functions, the accuracy associated with this method and approach can be considered sufficient for a qualitative study that reveals distinguishing cryoprotective characteristics of the modeled cryoprotectant solutions.

4. Conclusions

The present work shows a potential in application of the classical molecular dynamics for investigation of cryoprotective mechanisms related to prevention of recrystallization. The method qualitatively distinguished effects of different cryoprotectant solutions on the thermal stability of ice nuclei in the unfrozen portions of solutions at non-cryogenic temperatures. The results from the RDF and RMSD calculations demonstrated that the crowding of spherical compact Ficoll 70 molecules is an efficient approach to minimizing recrystallization during storage and warming, as well as to lowering the activity of liquid water molecules. These results qualitatively explained the observation from our previous cell cryopreservation experiments.

Acknowledgement

Support for this work by the U.S. National Science Foundation under grant number CBET-1404482 (YM and YZ), National Institute of Health under grant number 1R43OD020163 (XH) and the University of Missouri FastTrack Award 2017 (XH) is gratefully acknowledged.

Conflict of interest

The intellectual property related to this technology belongs to the University of Missouri, and a PCT patent application (PCT/ US2017/032606) has been filed. None of the other authors have any competing financial interests.

References

- J.M. Baust, C.W.L., R. VanBuskirk, J.G. Baust, Biobanking in the 21st century, in: F. K-B (Ed.), Advances in Experimental Medicine and Biology, Springer, Cham, 2015.
- [2] H.D. Blackburn, Biobanking genetic material for agricultural animal species, Annu. Rev. Anim. Biosci. 6 (1) (2018) 69–82.
- [3] M. Mendy, R.T. Lawlor, A.L. van Kappel, P.H.J. Riegman, F. Betsou, O.D. Cohen, M.K. Henderson, Biospecimens and biobanking in global health, Clin. Lab. Med. 38 (1) (2018) 183–207.
- [4] Z. He, K. Liu, J. Wang, Bioinspired materials for controlling ice nucleation, growth, and recrystallization, Acc. Chem. Res. (2018).
- [5] J.L. Chaytor, J.M. Tokarew, L.K. Wu, M. Leclère, R.Y. Tam, C.J. Capicciotti, L. Guolla, E. von Moos, C.S. Findlay, D.S. Allan, R.N. Ben, Inhibiting ice recrystallization and optimization of cell viability after cryopreservation, Glycobiology 22 (1) (2012) 123–133.
- [6] A. Baudot, V. Odagescu, Thermal properties of ethylene glycol aqueous solutions, Cryobiology 48 (3) (2004) 283–294.
- [7] M.a.M. Forsyth, D.R., Recrystallization revisited, CryoLetters 7(6) (1986) 367–378.

- [8] Y. Yuan, Y. Yang, Y. Tian, J. Park, A. Dai, R.M. Roberts, Y. Liu, X. Han, Efficient long-term cryopreservation of pluripotent stem cells at -80 °C, Sci. Rep. 6 (2016) 34476.
- [9] X.Y.Y. Han, R.M. Roberts, Inventor Cryopreservation Medium and Method to Prevent Recrystallization, 2017.
- [10] N.J. English, J.S. Tse, Massively parallel molecular dynamics simulation of formation of ice-crystallite precursors in supercooled water: incipientnucleation behavior and role of system size, Phys. Rev. E 92 (3) (2015) 032132.
- [11] J.Y. Yan, G.N. Patey, Molecular dynamics simulations of ice nucleation by electric fields, J. Phys. Chem. A 116 (26) (2012) 7057–7064.
- [12] E.A. Zheligovskaya, Molecular dynamics study of crystalline water ices, J. Struct. Chem. 49 (3) (2008) 459–471.
- [13] M. Matsumoto, S. Saito, I. Ohmine, Molecular dynamics simulation of the ice nucleation and growth process leading to water freezing, Nature 416 (2002) 409
- [14] U.S. Midya, S. Bandyopadhyay, Operation of Kelvin effect in the activities of an antifreeze protein: a molecular dynamics simulation study, J. Phys. Chem. B 122 (12) (2018) 3079–3087.
- [15] L. Weng, S.L. Stott, M. Toner, Molecular dynamics at the interface between ice and poly(vinyl alcohol) and ice recrystallization inhibition, Langmuir (2017).
- [16] M. Schauperl, M. Podewitz, T.S. Ortner, F. Waibl, A. Thoeny, T. Loerting, K.R. Liedl, Balance between hydration enthalpy and entropy is important for ice binding surfaces in antifreeze proteins, Sci. Rep. 7 (1) (2017) 11901.
- [17] V.I. Artyukhov, A.Y. Pulver, A. Peregudov, I. Artyuhov, Can xenon in water inhibit ice growth? Molecular dynamics of phase transitions in water–Xe system, J. Chem. Phys. 141 (3) (2014) 034503.
- [18] D. Corradini, E.G. Strekalova, H.E. Stanley, P. Gallo, Microscopic mechanism of protein cryopreservation in an aqueous solution with trehalose, Sci. Rep. 3 (2013) 1218.
- [19] P.B. Conrad, J.J. de Pablo, Computer simulation of the cryoprotectant disaccharide α,α-trehalose in aqueous solution, J. Phys. Chem. A 103 (20) (1999) 4049–4055.
- [20] Cerius, Forcefield Based Simulations, 2000. http://www.chem.cmu.edu/courses/09-560/docs/msi/ffbsim/FF_SimulTOC.doc.html (accessed 11-23 2015).
- [21] W.L. Jorgensen, D.S. Maxwell, J. Tirado-Rives, Development and testing of the Opls all-atom force field on conformational energetics and properties of organic liquids, J. Am. Chem. Soc. 118 (45) (1996) 11225–11236.
- [22] W. Ponder Jay, M. Richards Frederic, An efficient Newton-like method for molecular mechanics energy minimization of large molecules, J. Comput. Chem. 8 (7) (2004) 1016–1024.
- [23] W.H. Fissell, S. Manley, A. Dubnisheva, J. Glass, J. Magistrelli, A.N. Eldridge, A.J. Fleischman, A.L. Zydney, S. Roy, Ficoll is not a rigid sphere, Am. J. Physiol.-Renal Physiol. 293 (4) (2007) F1209-F1213.
- [24] W.L. Jorgensen, J. Tirado-Rives, The Opls [Optimized Potentials for Liquid Simulations] potential functions for proteins, energy minimizations for crystals of cyclic peptides and crambin, J. Am. Chem. Soc. 110 (6) (1988) 1657–1666
- [25] S.M.M. Andrew Jewett, 2015. http://www.moltemplate.org/ (accessed 11-23 2015).
- [26] D.H. Rasmussen, A.P. Mackenzie, Phase diagram for the system waterdimethylsulphoxide, Nature 220 (1968) 1315.
- [27] F.W. Kleinhans, P. Mazur, Comparison of actual vs. synthesized ternary phase diagrams for solutes of cryobiological interest, Cryobiology 54 (2) (2007) 212– 222.
- [28] X. Han, Y. Liu, J.K. Critser, Determination of the quaternary phase diagram of the water-ethylene glycol-sucrose-nacl system and a comparison between two theoretical methods for synthetic phase diagrams, Cryobiology 61 (1) (2010) 52–57.
- [29] S. Plimpton, Fast parallel algorithms for short-range molecular dynamics, J. Comput. Phys. 117 (1) (1995) 1–19.
- [30] W. Humphrey, A. Dalke, K. Schulten, Vmd: visual molecular dynamics, J. Mol. Graph. 14 (1) (1996) 33–38.
- [31] G. Todde, C. Whitman, S. Hovmöller, A. Laaksonen, Induced ice melting by the snow flea antifreeze protein from molecular dynamics simulations, J. Phys. Chem. B 118 (47) (2014) 13527–13534.
- [32] M. Chaplin, Water Structure and Science, 2015. http://www1.lsbu.ac.uk/water/hexagonal_ice.html (accessed 11-24 2015).
- [33] R.G. Pereyra, I. Szleifer, M.A. Carignano, Temperature dependence of ice critical nucleus size, J. Chem. Phys. 135 (3) (2011) 034508.
- [34] B.H. Zimm, The scattering of light and the radial distribution function of high polymer solutions, J. Chem. Phys. 16 (12) (1948) 1093–1099.
 [35] L. Wang, J. Liu, G.-B. Zhou, Y.-P. Hou, J.-J. Li, S.-E. Zhu, Quantitative
- [35] L. Wang, J. Liu, G.-B. Zhou, Y.-P. Hou, J.-J. Li, S.-E. Zhu, Quantitative investigations on the effects of exposure durations to the combined cryoprotective agents on mouse oocyte vitrification procedures, Biol. Reprod. 85 (5) (2011) 884–894.